An Inhibitor of TRPV1 Channels Isolated from Funnel Web Spider Venom†

Tetsuya Kitaguchi and Kenton J. Swartz*

Molecular Physiology and Biophysics Section, Porter Neuroscience Research Center, National Institute of Neurological Disorders and Stroke, National Institutes of Health, Bethesda, Maryland 20892

Received July 27, 2005; Revised Manuscript Received September 23, 2005

ABSTRACT: Capsaicin receptor channels (TRPV1) are nonselective cation channels that integrate multiple noxious stimuli in sensory neurons. In an effort to identify new inhibitors of these channels we screened a venom library for activity against TRPV1 channels and found robust inhibitory activity in venom from *Agelenopsis aperta*, a north American funnel web spider. Fractionation of the venom using reversed-phase HPLC resulted in the purification of two acylpolyamine toxins, AG489 and AG505, which inhibit TRPV1 channels from the extracellular side of the membrane. The activity of AG489 was characterized further, and the toxin was found to inhibit TRPV1 channels with a K_i of 0.3 μM at −40 mV. Inhibition of TRPV1 channels by AG489 is strongly voltage-dependent, with relief of inhibition at positive voltages, consistent with the toxin inhibiting the channel through a pore-blocking mechanism. We used scanning mutagenesis throughout the TM5−TM6 linker, a region thought to form the outer pore of TRPV1 channels, to identify pore mutations that alter toxin affinity. Four mutants dramatically decrease toxin affinity and several mutants increase toxin affinity, consistent with the notion that the TM5−TM6 linker forms the outer vestibule of TRPV1 channels and that AG489 is a pore blocker.

The capsaicin receptor, also known as TRPV1, belongs to the transient receptor potential family of nonselective cation channels (*1*). TRPV1 is expressed predominantly by sensory neurons (*1*) and responds to noxious stimuli, including capsaicin (the pungent component of chilli peppers), heat, and acid (*2*). TRPV1 is thought to play a crucial role in temperature sensing and nociception (*3*) and has attracted attention as a molecular target for pain treatment (*4*). The TRPV1 channel is predicted to have six transmembrane segments with a pore loop between TM5 and TM6, an architecture that is related to that found in voltage-activated potassium channels (Figure 1A). Although the TM5−TM6 region is thought to contribute to forming the ion conduction pathway (*5*−*11*), relatively little is known about the structure of this region (*12*). Recently, several TRP[1] channels were reported to exhibit voltage-dependent gating (*13*), strengthening the notion that their architecture is similar to that of voltage-activated potassium channels.

Despite the important implications of TRPV1 channel inhibitors, only a few have been found so far. The anionic histochemical dye, ruthenium red, was the first TRPV1 inhibitor described (*14*, *15*). Ruthenium red probably inhibits TRPV1 channels through a pore-blocking mechanism because inhibition is voltage-dependent, capsaicin-independent, and rather nonselective. The first described competitive antagonist of TRPV1 is capsazepine (*16*, *17*), and the first antagonist from natural sources is thapsigargin (*18*), an alkyloid derived from the mediterranean plant *Thapsia garganica* and a well-known inhibitor of the sarcoendoplasmic reticulum Ca^{2+}-ATPases. Yohimbin, an α2-adrenoceptor antagonist from the bark of the *Pausinystalia yohimbe* tree, and dynorphin, an opioid receptor agonist, have also been shown to inhibit TRPV1 channels (*18*, *19*), presumably

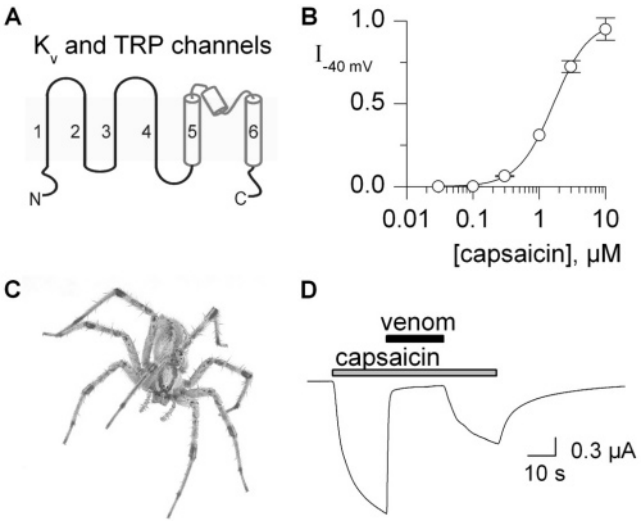

FIGURE 1: Activity of *A. aperta* venom on TRPV1 channels. (A) Proposed membrane folding diagram for TRP and K_v channels. (B) Dose−response curve for capsaicin activation of TRPV1. Membrane current was measured at −40 mV and normalized to the response to 10 μM capsaicin. Data points are the mean ± SEM for six measurements at each concentration. The smooth curve is a fit of the Hill equation to the data with $EC_{50} = 1.6\ \mu M$ and $n = 1.6$. (C) Photograph of the *A. aperta* spider. (Courtesy of Chuck Kristensen, Spider Pharm, Yarnell, AZ.) (D) Current activated by capsaicin (1 μM) and its inhibition by a 1:100 dilution of *A. aperta* venom. The holding potential is −40 mV.

† This research was supported by the Intramural Research Program of the NINDS, NIH.

* To whom correspondence should be addressed at the National Institutes of Health, 35 Convent Drive, 3B 215, MSC 3701, Bethesda, MD 20892. Phone: 301-435-5652. Fax: 301-435-5666. E-mail: swartzk@ninds.nih.gov.

[1] Abbreviations: TRP, transient receptor potential; HPLC, high-performance liquid chromatography; TFA, trifluoroacetic acid.

10.1021/bi051494l
Published on Web 11/04/2005

through second messenger pathways.

We set out to identify new inhibitors of TRPV1 channels, motivated by their possible utility in pain management and as tools for studying the structure and function of TRP channels. We began by screening venom from poisonous animals for activity against the TRPV1 channel expressed in *Xenopus* oocytes and found particularly robust inhibitory activity in venom from *Agelenopsis aperta*, a north American funnel web spider. This venom contains both protein and acylpolyamine toxins and has been a rich source of ion channel inhibitors (*20*). Here we describe the purification, biochemical analysis, and initial biophysical characterization of an acylpolyamine toxin that inhibits TRPV1 channels.

EXPERIMENTAL PROCEDURES

Materials. Capsaicin, PhTx-343, spermine, spermidine, putrescine, and tryptophan were purchased from Sigma-Aldrich (St. Louis, MO). JSTX-3 was from Wako Pure Chemical Industries (Osaka, Japan), and *A. aperta* venom was from Spider Pharm (Yarnell, AZ). Stock solutions of capsaicin (10 mM) and PhTx-343 (1 mM) were in ethanol and methanol, respectively, and all other stocks were in water.

Reversed-Phase HPLC and Mass Spectrometry. Venom was diluted 10−50-fold into 0.1% TFA in H_2O, clarified by centrifugation, and filtered through 0.2 μm acrodisk filters (Gelman Sciences, Ann Arbor, MI). The resulting supernatant was fractionated in two steps using a Beckman analytical gradient reversed-phase HPLC with either a Beckmann C18 column (4.6 mm × 25 cm, 5 μm, 80 Å) or a Vydac C18 column (4.6 mm × 25 cm, 5 μm, 300 Å). Separation and gradient conditions are detailed in the legend to Figure 2. Following purification, the concentrations of AG489 or AG505 were determined by absorbance at 280 nm using the extinction coefficient for tryptophan ($A_{280} = 5690\ M^{-1}\ cm^{-1}$) (*21*).

For mass spectrometric analysis, samples were introduced and analyzed on a Waters 1525μ binary pump equipped with a Waters 2777 sample manager that was connected online to an orthogonal ESI-TOF mass spectrometer (Micromass LCT Premier; Waters, Milford, ME). The mobile phase for the direct introduction of the sample contained 0.08% formic acid and 60% acetonitrile in water.

Molecular Biology and Channel Expression. All experiments were performed using the rat TRPV1 channel subcloned into pGEM-HE (*22*). Point mutations were generated through sequential PCR or the QuikChange site-directed mutagenesis kit II (Stratagene, Cedar Creek, TX), and all mutations were verified by automated DNA sequencing. Plasmids were linearized with *Not*I, and cRNAs were transcribed with T7 RNA polymerase. *Xenopus laevis* oocytes were removed surgically and incubated with agitation for 60−90 min in solution containing (in mM) 82.5 NaCl, 2.5 KCl, 1 $MgCl_2$, 5 HEPES, and 2 mg/mL collagenase, pH 7.6, with NaOH. Defolliculated oocytes were injected with cRNA and incubated at 17 °C in a solution containing (in mM) 96 NaCl, 2 KCl, 1 $MgCl_2$, 1.8 $CaCl_2$, 5 HEPES, and 50 μg/mL gentamicin, pH 7.6, with NaOH for 1−6 days before electrophysiological recording.

Electrophysiological Recording. Macroscopic ionic currents were recorded under voltage clamp using an OC-725C two-electrode voltage clamp amplifier (Warner Instrument Corp., Hamden, CT). When measuring capsaicin-activated currents at −40 mV, data were filtered at 50 Hz (8-pole Bessel) and digitized at 200 Hz using a Digidata 1321A interface board and pCLAMP 9 software (Axon Instruments). For experiments in which membrane voltage was varied using step protocols (Figure 4), filter frequency was 1 kHz and digitization frequency was 5 kHz. The recording solution contained (in mM) 100 NaCl, 5 HEPES, 1 $MgCl_2$, and 0.3 $BaCl_2$, pH 7.6.

RESULTS AND DISCUSSION

We began screening for activity against TRPV1 by expressing the channel in *Xenopus* oocytes, using capsaicin to activate the channel at a holding voltage of −40 mV. The concentration dependence for capsaicin activation of the channel is shown in Figure 1B, with half-maximal activation occurring at 1.6 μM, similar to what has been reported previously (*1*). We screened 44 venoms from scorpions, cone snails, spiders, snakes, and frogs for activity against the TRPV1 channel by adding diluted venom to the extracellular bath solution after activation of the channel with 1 μM capsaicin. Although a number of different venoms contain both stimulatory and inhibitory activity, the venom from *A. aperta* produces a particularly robust inhibitory effect on currents activated by capsaicin (Figure 1C,D). Addition of *A. aperta* venom diluted 100-fold into recording solution produces nearly complete inhibition of capsaicin-activated currents.

To purify the inhibitory activity, we fractioned *A. aperta* venom using reversed-phase HPLC with water−acetonitrile gradients, testing individual peaks for activity against the TRPV1 channel. The HPLC fractionation of crude venom results in a chromatogram that contains two predominant clusters of peaks (Figure 2A). It has been previously documented that the venom components eluting between 15 and 25 min are primarily acylpolyamine toxins, whereas the components eluting between 40 and 50 min are primarily protein toxins (*20*, *23*−*25*). When these fractions are examined for activity against TRPV1, inhibitory activity is observed for the cluster of peaks corresponding to polyamines (indicated by the gray shading in Figure 2A). The chromatogram in Figure 2B shows subsequent fractionation of polyamines using a modified separation procedure, which yields two peaks with robust inhibitory activity. The chromatographic signature observed in Figure 2B suggests that the active components correspond to AG505 and AG489 (*23*, *25*), two previously isolated toxins of known structure (Figure 2D). The identity of the two purified acylpolyamine toxins was confirmed by mass spectrometric analysis, which yielded masses of 490.4 for AG489 and 506.4 for AG505, consistent with previous determinations (*26*, *27*). Our subsequent experimentation focuses on AG489 because this toxin is more abundant in venom and both toxins exhibit similar inhibitory activity (see Figure 5).

To investigate the concentration dependence for inhibition by AG489, different concentrations of the toxin were applied to the extracellular solution after the channel was activated by 1 μM capsaicin at a holding voltage of −40 mV. At a concentration of 10 μM, AG489 completely inhibits current at −40 mV, requiring about 20 s to reach equilibrium (Figure

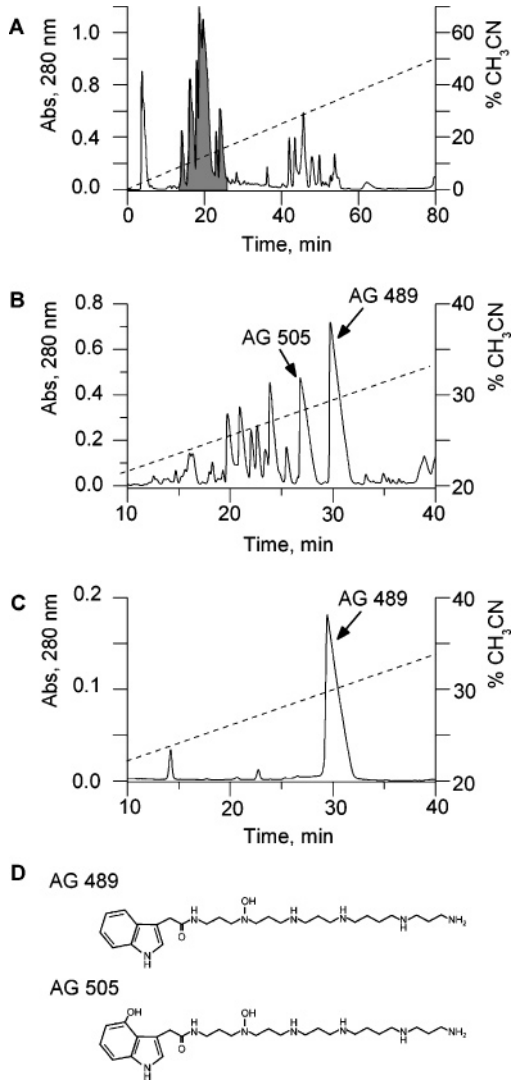

FIGURE 2: Purification of TRPV1 channel inhibitor *A. aperta* venom. (A) Reversed-phase HPLC chromatogram for 10 μL of neat *A. aperta* venom. Venom was fractioned on a Beckmann C18 (4.6 mm $\times$ 25 cm, 5 μm, 80 Å) column using a gradient from water to acetonitrile. A linear gradient was employed from 0% to 50% mobile phase B over 80 min, where mobile phase A was 0.1% TFA in water and mobile phase B was 0.08% TFA in acetonitrile. Inhibitory activity was found throughout the region indicated by the gray shading. (B) The active fractions in (A) were fractioned a second time using reversed-phase HPLC on a Vydac C18 (4.6 mm $\times$ 25 cm, 5 μm, 300 Å). A linear gradient was employed from 20% to 40% mobile phase B over 60 min, where mobile phase A was 0.1% heptafluorobutyric acid (HFBA) in water and mobile phase B was 0.08% HFBA in acetonitrile. (C) Chromatogram of pure AG489 using the same column and protocol as in (B). (D) Structures of AG489 and AG505 (*26*, *27*).

3A). Following removal of the toxin from the recording chamber the current at -40 mV recovers along a significantly slower time course (Figure 3A). The inhibition seen with lower concentrations of AG489 develops more slowly and produces less than complete inhibition (Figure 3B). The relatively slow kinetics for the onset of inhibition makes it difficult to ascertain whether equilibrium had been achieved at concentrations below 0.3 μM. Despite this limitation, the relationship between fractional inhibition and toxin concentration (0.3$-$30 μM) could be well described assuming a 1:1 interaction between toxin and channel, with an apparent K_i of 0.3 μM (Figure 3B).

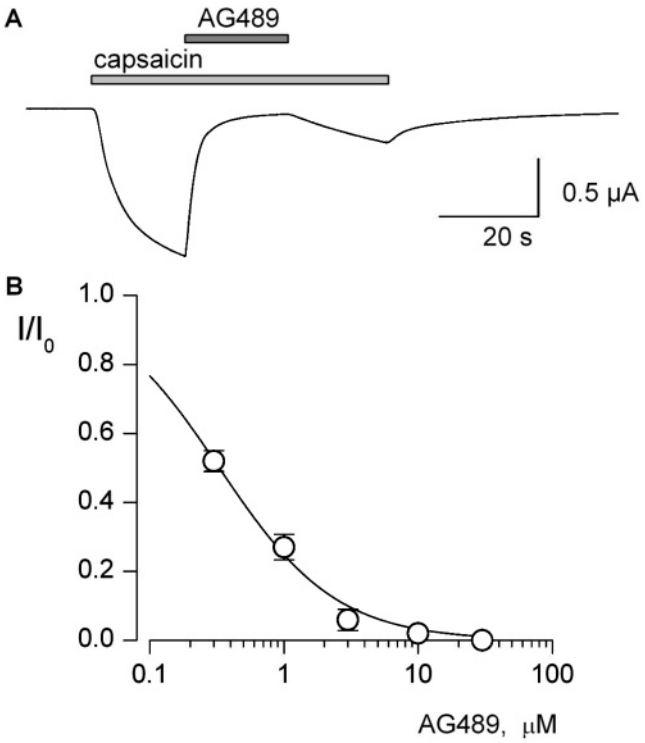

FIGURE 3: Inhibition of the TRPV1 channel by AG489. (A) Activation of TRPV1 channels by 1 μM capsaicin and subsequent inhibition by 10 μM AG489. The holding voltage is -40 mV. (B) Concentration dependence for inhibition by AG489. Ionic current was elicited by 1 μM capsaicin at -40 mV. I/I_0 is the fraction of uninhibited current. The solid line is a fit of $I/I_0 = 1 - ([AG489]/[AG489] + K_i)$ to the data with $K_i = 0.3$ μM. Each point represents the mean $\pm$ SEM for five to eight measurements.

Polyamines are known to interact with ion conduction pores in several types of cation channels, including potassium channels (*28*, *29*), cyclic nucleotide gated channels (*30*), glutamate receptor channels (*31*), nicotinic acetylcholine receptor channels (*32*), and both TRPM4 and TRPM7 channels (*33*, *34*). In most cases polyamines inhibit from the intracellular side of the membrane, and inhibition is strongly voltage-dependent. In the case of potassium channels there is extensive evidence that polyamines inhibit by a pore-blocking mechanism (*28*). To ascertain whether AG489 works through a similar mechanism, we examined whether inhibition by AG489 was voltage-dependent. TRPV1 was activated with 1 μM capsaicin, and voltage steps were applied between -100 and $+100$ mV from a holding voltage of -10 mV. As shown in Figure 4A, 10 μM AG489 inhibits the TRPV1 channel at -40 mV to a much greater extent when compared to $+40$ mV. Capsaicin-activated currents are plotted in Figure 4B for a range of different voltages in both the presence and absence of AG489, and the fractional inhibition is plotted against membrane voltage in Figure 4C. Fitting of a Boltzmann function to the relief of inhibition at voltages positive to -25 mV yields a slope factor of 12 mV, corresponding to a $z\delta$ of about 2, where z is the amount of charge moving through a fraction (δ) of the membrane electric field. The relatively small decrease in fractional inhibition at membrane voltages negative to -50 mV is not due to permeation of the toxin (e.g., refs *30* and *35*) but results from a negative slope in the current$-$voltage relation under control conditions, presumably reflecting a voltage dependence to the open probability of the channel (*13*). When

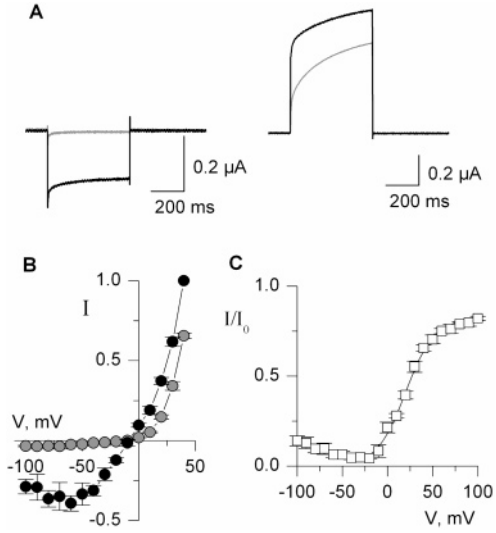

FIGURE 4: Voltage-dependent inhibition of TRPV1 by AG489. (A) The TRPV1 channel was activated by 1 μM capsaicin in the absence (black) and presence of 10 μM AG489 (gray). Voltage steps are from a holding voltage of −10 to −40 mV (left panel) or +40 mV (right panel). Leak and linear capacitive identified in the absence of capsaicin have been subtracted. (B) Voltage dependence of AG489 inhibition. Currents measured in the absence (black circles) or presence (gray circles) of 10 μM AG489 measured at the end of the voltage step, normalized to the current amplitude elicited by stepping to +40 mV in the absence of toxin. The holding voltage was −40 mV. Data points are the mean ± SEM for seven measurements. (C) Fraction of current uninhibited by AG489 plotted against membrane voltage. Data points are the mean ± SEM for seven measurements. The smooth curve is a fit of a single Boltzmann function to the data between −25 and +100 mV with a slope factor of 12 mV.

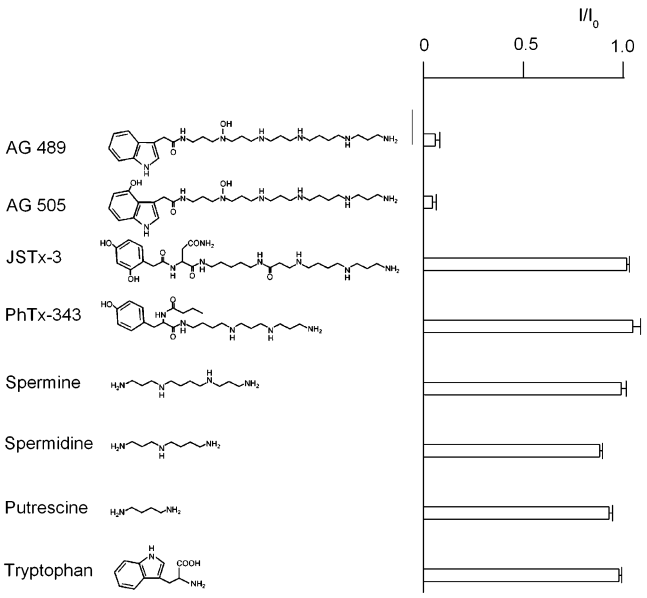

FIGURE 5: Comparison of the effects of polyamines on the TRPV1 channel. Currents were activated by capsaicin (1 μM) at −40 mV prior to extracellular application of the test polyamine. I/I_0 is the fraction of uninhibited current. Each bar represents the mean ± SEM for between three and six measurements. Polyamines were tested at the following concentrations: AG489 (3 μM), AG505 (3 μM), JSTX-3 (1 μM), PhTx-343 (30 μM), spermine (1 mM), spermidine (1 mM), putrescine (10 mM), and tryptophan (200 μM).

considered in the context of mechanistic experiments in other types of cation channels, the voltage dependence of inhibition by AG489 is consistent with a pore-blocking mechanism.

To further establish that the inhibitory mechanism of AG489 does not involve interfering with capsaicin activation of TRPV1 channels per se, we compared inhibition by AG489 when the channel was activated by 1 and 10 μM capsaicin. The fractions of uninhibited current seen with 1, 3, and 10 μM AG489 are 0.26 ± 0.04, 0.08 ± 0.03, and 0.04 ± 0.005 when the channel is activated by 10 μM capsaicin, which are indistinguishable from corresponding values of 0.27 ± 0.04, 0.06 ± 0.03, and 0.02 ± 0.002 when the channel is activated by 1 μM capsaicin.

AG489 is an indole-containing polyamine that was first discovered to paralyze adult house flies and inhibit excitatory postsynaptic potentials at glutamatergic neuromuscular synapses (*23*, *25*). The use dependence of postsynaptic inhibition described in the fly (*23*) supports the notion that AG489 inhibits through a pore-blocking mechanism. Subsequent studies showed that AG489 inhibits the NMDA (*N*-methyl-D-aspartate) subtype of glutamate receptor channels (*36*−*38*). Since NMDA receptor channels are inhibited by several different polyamines (*38*−*41*), we investigated whether other polyamines also inhibit the TRPV1 channel. Although previous studies have found that AG489, AG505, JSTX-3, and PhTx-343 inhibit NMDA receptor channels, we find that JSTX-3 (1 μM) and PhTx-343 (30 μM) have no significant effect when applied to the extracellular side of TRPV1 channels (Figure 5). In addition, we find that spermine (1 mM), spermidine (1 mM), and putrescine (10 mM) have little or no effect on TRPV1 channels. These results suggest that TRPV1 is rather selective for indole-containing polyamines. This contrasts with data for TRPM7, which is inhibited by putrescine, spermidine, spermine, and PhTx-343 from the extracellular side of the membrane (*33*), highlighting a significant difference in the polyamine sensitivities of TRPV1 and TRPM7.

Given the likelihood that AG489 inhibits TRPV1 through a pore-blocking mechanism, we examined whether mutations within the proposed pore-forming region of TRPV1 alter inhibition by the toxin. The architectural relatedness of potassium and TRP channels, as well as the discovery of mutants affecting ion permeation in TRP channels (*5*−*11*), supports the notion that the TM5−TM6 linker forms the external vestibule of the ion conduction pore. Figure 6A shows a sequence alignment between the putative pore region in TRPV1 and the KcsA potassium channel (*42*, *43*). We tryptophan scanned this region, mutating 25 consecutive residues to tryptophan. Of these mutants, 15 result in channel expression that can be readily studied using electrophysiolgical techniques, whereas 10 produce little or no capasaicin-activated current and were not studied further. One residue in this region (D646) was also mutated to asparagine since this mutant was previously reported to alter inhibition by ruthenium red (*5*), and the D646W mutant did not yield functional channels. Figure 6B shows a summary of the tryptophan scan, where $\ln(K_i^{mut}/K_i^{Wt})$ is plotted for each functional mutant. Interestingly, the nonfunctional mutants are clustered together near the middle of the region mutated, which corresponds to a region of potassium channels (the signature sequence) that is similarly intolerant to substitution (*44*). Mutation of multiple residues flanking this intolerant region results in channels that exhibit diminished or enhanced sensitivity to AG489. The residues where mutations decrease sensitivity to the toxin are uniformly polar in the Wt channel,

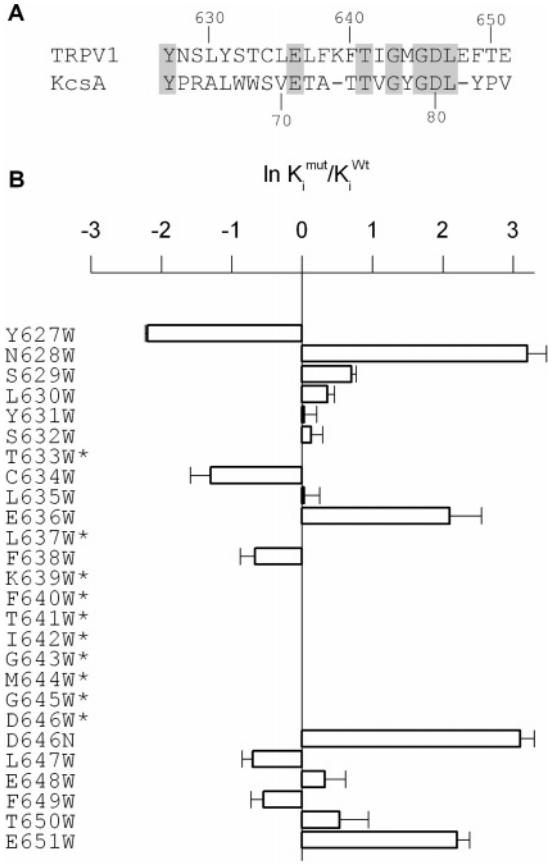

FIGURE 6: Tryptophan scanning mutagenesis of the TM5−TM6 linker region of TRPV1. (A) Sequence alignment between the putative pore region of TRPV1 and the pore of the KcsA potassium channel. Identical residues are in gray boxes. (B) Plot of $\ln(K_i^{mut}/K_i^{Wt})$ for each mutant in TM5−TM6. Currents were activated by 10 μM capsaicin using a holding voltage of −40 mV. Concentrations for AG489 were between 1 and 30 μM, with three to six determinations at each concentration. Asterisks designate those mutants that gave rise to little or no capsaicin-activated current at −40 mV.

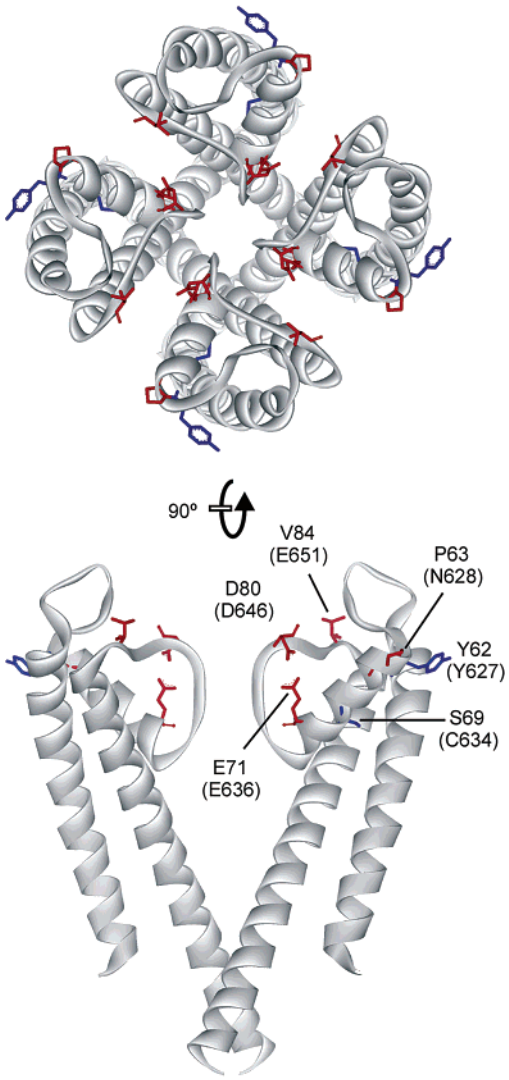

FIGURE 7: Perturbations in AG489 affinity mapped onto the structure of the KcsA potassium channel. Residues in red are P63, E71, D80, and V84, which correspond to N628, E636, D646, and E651 in TRPV1, where mutations weaken toxin affinity. Residues in blue are Y62 and S69, which correspond to Y627 and C634 in TRPV1, where mutations enhance toxin affinity. The top structure is a view of the tetrameric channel from the extracellular side, whereas the bottom structure is a side view with front and back subunits removed for clarity. Structures drawn using DS Viewer Pro 5.0 (Accelrys); PDB accession number 1K4C.

including N628, E636, D646, and E651. In contrast, the residues where mutation to tryptophan enhances sensitivity to the toxin are all hydrophobic in the Wt channel, including Y627 and C634 and to a lesser extent F638, L647, and F649. Figure 7 shows a mapping of these mutagenesis results onto the X-ray structure of the KcsA potassium channel, where the positions exhibiting decreased sensitivity are colored red and those with enhanced sensitivity are colored blue. Although these results clearly support the notion that the TM5−TM6 linker contributes to forming the external pore region in TRP channels, they also give the impression that the structure of the outer pore in TRP and potassium channels may differ in substantial ways. A number of the largest perturbations in AG489 binding to TRPV1, for example, occur for residues that in the structure of the potassium channel are far from the central ion conduction pathway.

In conclusion, we have isolated and characterized an acylpolyamine toxin that inhibits the TRPV1 channel. The voltage dependence for inhibition by AG489, together with previous studies of polyamine inhibitors of cation channels, suggests that the toxin inhibits by blocking the ion conduction pathway. Mutagenesis of the TM5−TM6 linker region suggests that the general architecture of the pore region in TRPV1 is related to that found in potassium channels.

ACKNOWLEDGMENT

We thank Dr. David Julius for the rTRPV1 plasmid and Drs. Howard Jaffe and Sonja Hess for mass spectrometry. We also thank Shai Silberberg and members of the Swartz laboratory for helpful discussions and critique of the manuscript.

REFERENCES

1. Caterina, M. J., Schumacher, M. A., Tominaga, M., Rosen, T. A., Levine, J. D., and Julius, D. (1997) The capsaicin receptor: a heat-activated ion channel in the pain pathway, *Nature 389*, 816−824.
2. Tominaga, M., Caterina, M. J., Malmberg, A. B., Rosen, T. A., Gilbert, H., Skinner, K., Raumann, B. E., Basbaum, A. I., and Julius, D. (1998) The cloned capsaicin receptor integrates multiple pain-producing stimuli, *Neuron 21*, 531−543.
3. Caterina, M. J., Leffler, A., Malmberg, A. B., Martin, W. J., Trafton, J., Petersen-Zeitz, K. R., Koltzenburg, M., Basbaum, A.

I., and Julius, D. (2000) Impaired nociception and pain sensation in mice lacking the capsaicin receptor, *Science 288*, 306−313.
4. Szallasi, A., and Appendino, G. (2004) Vanilloid receptor TRPV1 antagonists as the next generation of painkillers. Are we putting the cart before the horse?, *J. Med. Chem. 47*, 2717−2723.
5. Garcia-Martinez, C., Morenilla-Palao, C., Planells-Cases, R., Merino, J. M., and Ferrer-Montiel, A. (2000) Identification of an aspartic residue in the P-loop of the vanilloid receptor that modulates pore properties, *J. Biol. Chem. 275*, 32552−32558.
6. Hoenderop, J. G., Voets, T., Hoefs, S., Weidema, F., Prenen, J., Nilius, B., and Bindels, R. J. (2003) Homo- and heterotetrameric architecture of the epithelial Ca^{2+} channels TRPV5 and TRPV6, *EMBO J. 22*, 776−785.
7. Jung, S., Muhle, A., Schaefer, M., Strotmann, R., Schultz, G., and Plant, T. D. (2003) Lanthanides potentiate TRPC5 currents by an action at extracellular sites close to the pore mouth, *J. Biol. Chem. 278*, 3562−3571.
8. Liu, X., Singh, B. B., and Ambudkar, I. S. (2003) TRPC1 is required for functional store-operated Ca^{2+} channels. Role of acidic amino acid residues in the S5−S6 region, *J. Biol. Chem. 278*, 11337−11343.
9. Nilius, B., Vennekens, R., Prenen, J., Hoenderop, J. G., Droogmans, G., and Bindels, R. J. (2001) The single pore residue Asp542 determines Ca^{2+} permeation and Mg^{2+} block of the epithelial Ca^{2+} channel, *J. Biol. Chem. 276*, 1020−1025.
10. Voets, T., Janssens, A., Droogmans, G., and Nilius, B. (2004) Outer pore architecture of a Ca^{2+}-selective TRP channel, *J. Biol. Chem. 279*, 15223−15230.
11. Voets, T., Prenen, J., Vriens, J., Watanabe, H., Janssens, A., Wissenbach, U., Bodding, M., Droogmans, G., and Nilius, B. (2002) Molecular determinants of permeation through the cation channel TRPV4,. *J. Biol. Chem. 277*, 33704−33710.
12. Voets, T., and Nilius, B. (2003) The pore of TRP channels: trivial or neglected?, *Cell Calcium 33*, 299−302.
13. Voets, T., Droogmans, G., Wissenbach, U., Janssens, A., Flockerzi, V., and Nilius, B. (2004) The principle of temperature-dependent gating in cold- and heat-sensitive TRP channels, *Nature 430*, 748−754.
14. Maggi, C. A., Patacchini, R., Santicioli, P., Giuliani, S., Geppetti, P., and Meli, A. (1988) Protective action of ruthenium red toward capsaicin desensitization of sensory fibers, *Neurosci. Lett. 88*, 201−205.
15. Amann, R., and Maggi, C. A. (1991) Ruthenium red as a capsaicin antagonist, *Life Sci. 49*, 849−856.
16. Walpole, C. S., Bevan, S., Bovermann, G., Boelsterli, J. J., Breckenridge, R., Davies, J. W., Hughes, G. A., James, I., Oberer, L., Winter, J., et al. (1994) The discovery of capsazepine, the first competitive antagonist of the sensory neuron excitants capsaicin and resiniferatoxin, *J. Med. Chem. 37*, 1942−1954.
17. Dickenson, A. H., and Dray, A. (1991) Selective antagonism of capsaicin by capsazepine: evidence for a spinal receptor site in capsaicin-induced antinociception, *Br. J. Pharmacol. 104*, 1045−1049.
18. Toth, A., Kedei, N., Szabo, T., Wang, Y., and Blumberg, P. M. (2002) Thapsigargin binds to and inhibits the cloned vanilloid receptor-1, *Biochem. Biophys. Res. Commun. 293*, 777−782.
19. Planells-Cases, R., Aracil, A., Merino, J. M., Gallar, J., Perez-Paya, E., Belmonte, C., Gonzalez-Ros, J. M., and Ferrer-Montiel, A. V. (2000) Arginine-rich peptides are blockers of VR-1 channels with analgesic activity, *FEBS Lett. 481*, 131−136.
20. Adams, M. E. (2004) Agatoxins: ion channel specific toxins from the American funnel web spider, *Agelenopsis aperta*, *Toxicon 43*, 509−525.
21. Gill, S. C., and von Hippel, P. H. (1989) Calculation of protein extinction coefficients from amino acid sequence data, *Anal. Biochem. 182*, 319−326.
22. Liman, E. R., Tytgat, J., and Hess, P. (1992) Subunit stoichiometry of a mammalian K^+ channel determined by construction of multimeric cDNAs, *Neuron 9*, 861−871.
23. Adams, M. E., Herold, E. E., and Venema, V. J. (1989) Two classes of channel-specific toxins from funnel web spider venom, *J. Comp. Physiol., A 164*, 333−342.
24. Mintz, I. M., Venema, V. J., Swiderek, K. M., Lee, T. D., Bean, B. P., and Adams, M. E. (1992) P-type calcium channels blocked by the spider toxin omega-Aga-IVA, *Nature 355*, 827−829.
25. Skinner, W. S., Adams, M. E., Quistad, G. B., Kataoka, H., Cesarin, B. J., Enderlin, F. E., and Schooley, D. A. (1989) Purification and characterization of two classes of neurotoxins from the funnel web spider, *Agelenopsis aperta*, *J. Biol. Chem. 264*, 2150−2155.
26. Jasys, V. J., Kelbaugh, P. R., Nason, D. M., Phillips, D., Rosnack, K. J., Saccomano, N. A., Stroh, J. G., and Volkmann, R. A. (1990) Isolation, structure elucidation, and synthesis of novel hydroxylamine-containing polyamines from the venom of the *Agelenopsis aperta* spider, *J. Am. Chem. Soc. 112*, 6696−6704.
27. Quistad, G. B., Suwanrumpha, S., Jarema, M. A., Shapiro, M. J., Skinner, W. S., Jamieson, G. C., Lui, A., and Fu, E. W. (1990) Structures of paralytic acylpolyamines from the spider *Agelenopsis aperta*, *Biochem. Biophys. Res. Commun. 169*, 51−56.
28. Lu, Z. (2004) Mechanism of rectification in inward-rectifier K^+ channels. *Annu. Rev. Physiol. 66*, 103−129.
29. Lopatin, A. N., Makhina, E. N., and Nichols, C. G. (1994) Potassium channel block by cytoplasmic polyamines as the mechanism of intrinsic rectification, *Nature 372*, 366−369.
30. Guo, D., and Lu, Z. (2000) Mechanism of cGMP-gated channel block by intracellular polyamines, *J. Gen. Physiol. 115*, 783−798.
31. Panchenko, V. A., Glasser, C. R., and Mayer, M. L. (2001) Structural similarities between glutamate receptor channels and K(+) channels examined by scanning mutagenesis, *J. Gen. Physiol. 117*, 345−360.
32. Liu, M., Nakazawa, K., Inoue, K., and Ohno, Y. (1997) Potent and voltage-dependent block by philanthotoxin-343 of neuronal nicotinic receptor/channels in PC12 cells, *Br. J. Pharmacol. 122*, 379−385.
33. Kerschbaum, H. H., Kozak, J. A., and Cahalan, M. D. (2003) Polyvalent cations as permeant probes of MIC and TRPM7 pores, *Biophys. J. 84*, 2293−2305.
34. Nilius, B., Prenen, J., Voets, T., and Droogmans, G. (2004) Intracellular nucleotides and polyamines inhibit the Ca^{2+}-activated cation channel TRPM4b, *Pfluegers Arch. 448*, 70−75.
35. Lu, Z., and Ding, L. (1999) Blockade of a retinal cGMP-gated channel by polyamines, *J. Gen. Physiol. 113*, 35−43.
36. Williams, K. (1993) Effects of *Agelenopsis aperta* toxins on the *N*-methyl-D-aspartate receptor: polyamine-like and high-affinity antagonist actions, *J. Pharmacol. Exp. Ther. 266*, 231−236.
37. Kiskin, N. I., Chizhmakov, I. V., Tsyndrenko, A., Mueller, A. L., Jackson, H., and Krishtal, O. A. (1992) A highly potent and selective *N*-methyl-D-aspartate receptor antagonist from the venom of the *Agelenopsis aperta* spider, *Neuroscience 51*, 11−18.
38. Parks, T. N., Mueller, A. L., Artman, L. D., Albensi, B. C., Nemeth, E. F., Jackson, H., Jasys, V. J., Saccomano, N. A., and Volkmann, R. A. (1991) Arylamine toxins from funnel-web spider (*Agelenopsis aperta*) venom antagonize *N*-methyl-D-aspartate receptor function in mammalian brain, *J. Biol. Chem. 266*, 21523−21529.
39. Ragsdale, D., Gant, D. B., Anis, N. A., Eldefrawi, A. T., Eldefrawi, M. E., Konno, K., and Miledi, R. (1989) Inhibition of rat brain glutamate receptors by philanthotoxin, *J. Pharmacol. Exp. Ther. 251*, 156−163.
40. Mueller, A. L., Albensi, B. C., Ganong, A. H., Reynolds, L. S., and Jackson, H. (1991) Arylamine spider toxins antagonize NMDA receptor-mediated synaptic transmission in rat hippocampal slices, *Synapse 9*, 244−250.
41. Draguhn, A., Jahn, W., and Witzemann, V. (1991) Argiotoxin636 inhibits NMDA-activated ion channels expressed in *Xenopus* oocytes, *Neurosci. Lett. 132*, 187−190.
42. Doyle, D. A., Morais Cabral, J., Pfuetzner, R. A., Kuo, A., Gulbis, J. M., Cohen, S. L., Chait, B. T., and MacKinnon, R. (1998) The structure of the potassium channel: molecular basis of K^+ conduction and selectivity, *Science 280*, 69−77.
43. Zhou, Y., Morais-Cabral, J. H., Kaufman, A., and MacKinnon, R. (2001) Chemistry of ion coordination and hydration revealed by a K^+ channel-Fab complex at 2.0 Å resolution, *Nature 414*, 43−48.
44. Heginbotham, L., Lu, Z., Abramson, T., and MacKinnon, R. (1994) Mutations in the K^+ channel signature sequence, *Biophys. J. 66*, 1061−1067.

BI051494L